Notes #3: Electroweak Baryogenesis

David Morrissey
August 11, 2017

Electroweak baryogenesis (EWBG) is a mechanism to create the baryogen asymmetry in the course of the electroweak phase transition [1, 2, 3, 4]. If the transition is strongly first order, it proceeds through the nucleation of bubbles of broken phase within the surrounding plasma of symmetric phase. These bubbles expand, collide, and coalesce until they eventually fill the entire universe. Baryon creation in EWBG occurs in the vicinity of the bubble walls, which provide a strong departure from thermodynamic equilibrium. Particle scattering off the bubble walls with C and CP violation can generate net chiral asymmetries (*e.g.* more left-handed quarks than right-handed quarks) which bias the sphaleron transitions outside the bubbles to create more baryons than antibaryons. Once baryons are created, they are quickly swept up into the interior of the expanding bubbles where they are effectively stable. These processes are illustrated in Fig. 1.

All the basic ingredients needed for EWBG are present in the SM, and initially it was hoped that this mechanism could explain the baryon asymmetry with known particle physics. Unfortunately, detailed calculations show that baryogenesis by EWBG within the SM fails for two reasons. First, the electroweak phase transition is not first order for the measured value of the Higgs boson mass, and thus it does not produce the electroweak bubbles needed for EWBG [5]. Second, the CP violation present in the SM from the CKM phase does not appear to be enough to allow the creation of the observed asymmetry, even if the phase transition were first-order [6, 7].

Electroweak baryogenesis can be viable in extensions of the SM with new physics near the weak scale. The new states must couple significantly to the SM(-like) Higgs field in order to drive a strongly first-order phase transition. As a result, they often modify the production and decay properties of the Higgs boson. The new physics must also provide additional sources of CP violation connected to the Higgs. This can give rise to permanent electric dipole moments (EDMs) well above the level predicted by the SM alone. Both EWBG requirements also imply that at least some of the new physics must be near the weak scale, and thus it might be possible to detect it directly at the LHC. These arguments illustrate why EWBG is exciting and challenging: it can be tested thoroughly by current and upcoming experiments!

In these notes we give a short introduction to EWBG. We begin with an extremely brief review of quantum field theory at finite temperature. Next, we apply this machinery to the evolution of the Higgs field in the early universe and the related electroweak phase transition, and we discuss what is needed beyond the SM for a strongly first order electroweak phase transition. Finally, we present a mechanism for the creation of a baryon asymmetry in the vicinity of electroweak bubble walls. Some reviews of EWBG can be found in Refs. ([4, 8, 9, 10]).

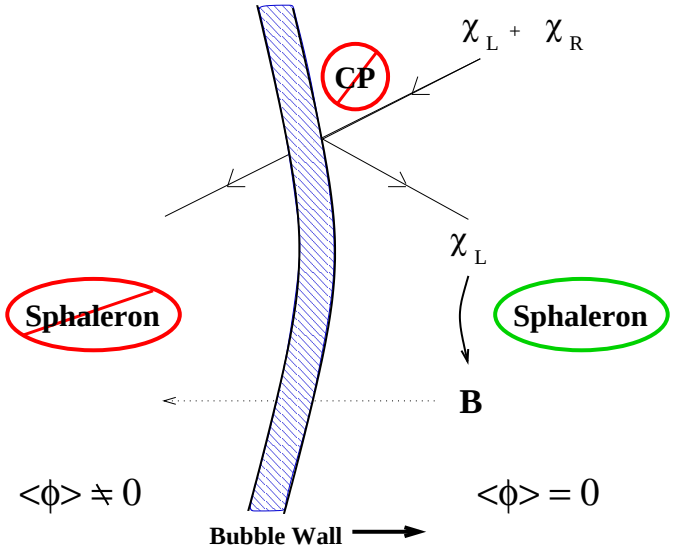

Figure 1: Schematic diagram of EWBG. The electroweak bubble wall separating the broken (left) and unbroken (right) phases is advancing from left to right. Fermion scattering off the wall with CP violation generates a chiral asymmetry that biases the fast sphaleron transitions outside the wall to create a net baryon charge. This charge is then swept up the advancing bubble into the broken phase where the sphaleron rate is exponentially suppressed.

1 QFT at Finite Temperature

Quantum field theory (QFT) is usually formulated (for particle physicists) with scattering in mind. Sets of well-separated particles enter from asymptotic past infinity ($t = -\infty$) travelling through otherwise empty space, collide with each other, and the collision products continue on to asymptotic future infinity ($t = +\infty$). This is appropriate for computing rates in particle colliders, but it can be a very poor approximation in the hot early universe, where the energetic background can play a very important role. In fact, the effects of the thermal background can even change the equilibrium state of the system. We discuss these topics here briefly. More detailed reviews can be found in Refs. [9, 12].

1.1 The Effective Potential at Zero Temperature

Before going thermal, let us start with a reminder of how one computes the ground state of a QFT at zero temperature. The key object for this is the (1PI) effective action, defined for a scalar field theory by [9, 13]

$$\Gamma[\phi_c] = \sum_{n=0}^{\infty} \frac{1}{n!} \left[\prod_{i=1}^{n} \int d^4x_i \; \phi_c(x_i) \right] \Gamma^{(n)}(x_1, \ldots, x_n) \; , \tag{1}$$

where $\phi_c(x)$ is a classical field and $\Gamma^{(n)}$ are the one-particle-irreducible (1PI) connected n-point Green's functions. This definition can also be expanded to theories with fermion and vector fields. The effective action has all sorts of interesting properties, of which the most important for us will be its role in giving the vacuum configuration of the theory.

With zero-momentum vacuum states in mind, let us expand the effective action in powers of derivatives [9, 13]

$$\Gamma[\phi_c] = \int d^4x \ \left[V_{eff}(\phi_c) + \frac{1}{2} Z(\phi_c)(\partial\phi_c)^2 + \dots \right] \ , \tag{2}$$

where the expression above defines the *effective potential*. Specializing to constant (spacetime independent) classical configurations, it is straightforward to show that

$$V_{eff}(\phi_c) = -\sum_n \frac{\phi_c^n}{n!} \widetilde{\Gamma}^{(n)}(p_i = 0) \ , \tag{3}$$

where $\widetilde{\Gamma}^{(n)}(p_i = 0)$ are the 1PI n-point functions in momentum space evaluated at $p_i \to 0$. This result provides a straightforward mechanism to compute the effective potential in peturbation theory. At tree-level, the 1PI n-point functions at zero momentum are the standard vertices for the theory, and thus the tree-level effective potential is just the classical potential. At the next order, we must sum all one loop diagrams with n external ϕ legs, and this provides the leading quantum correction to V_{eff}. It turns out that these diagrams can be summed into a very compact expression.

The physical interpretation of the effective potential $V_{eff}(\phi_c)$ is that it describes the vacuum energy density of the scalar theory with an implicit source term[1] for all normalizable vacuum states with [13, 15]

$$1 = \langle a|a\rangle \ , \qquad \phi_c = \langle a|\phi(x)|a\rangle \ . \tag{4}$$

It can be shown that the implicit source vanishes when

$$\frac{\partial V_{eff}}{\partial \phi_c} = 0 \ . \tag{5}$$

Since this is also the extremization condition with respect to ϕ_c, it follows that the the value of ϕ_c that minimizes $V_{eff}(\phi_c)$ corresponds to the vacuum configuration of the physical theory. Let us also emphasize that the interpretation of $V_{eff}(\phi_c)$ as a vacuum energy is only true for the original scalar theory at extrema.

Let us now turn to the Standard Model (SM) with tree-level Higgs potential

$$-\mathscr{L} \ \supset \ -\mu^2 H^\dagger H + \frac{\lambda}{2}(H^\dagger H)^2 \ , \tag{6}$$

with the Higgs doublet given by

$$H = \begin{pmatrix} G^+ \\ \phi + \frac{1}{\sqrt{2}}(h + iG^0) \end{pmatrix} \ , \tag{7}$$

[1] Adding a source $\int d^4x \, J(x)\phi(x)$ to the action shifts the location and energy of the vacuum of the theory.

where h corresponds to the physical Higgs boson and G^+ and G^0 are the Nambu-Goldstone modes. The effective potential in Landau gauge with $\overline{MS}$ renormalization is found to be

$$V_{eff}(\phi) = V_0(\phi) + V_1(\phi) + \dots \tag{8}$$

with the tree-level contribution

$$V_0(\phi) = -\mu^2\phi^2 + \frac{\lambda}{2}\phi^4 \ , \tag{9}$$

and the one-loop part

$$V_1(\phi) = \sum_i (-1)^{2s_i} g_i \, m_i^4 \left[\ln\left(\frac{m_i^2}{\overline{\mu}^2}\right) - C_i \right] \tag{10}$$

where $\overline{\mu}$ is the $\overline{MS}$ renormalization scale, $C_i = 3/2$ for the scalars and fermions and $C_i = 5/6$ for the vectors and the most important field dependent mass contributions are

$$\begin{array}{rll} h: & g_i = 1 & m_i^2 = -\mu^2\phi^2 + 3\lambda\phi^2 \\ G^0,\, G^+: & g_i = 1,2 & m_i^2 = -\mu^2 + \lambda\phi^2 \\ W: & g_i = 6 & m_i^2 = g^2\phi^2/2 \\ Z: & g_i = 3 & m_i^2 = (g^2 + g'^2)\phi^2/2 \\ t: & g_i = 12 & m_i^2 = y_t^2\phi^2 \end{array} \tag{11}$$

These loop corrections modify the depth of the standard electroweak minimum slightly, but they do not change the quantitative result of electroweak symmetry breaking there, with $\phi \simeq 174$ GeV at the minimum.

1.2 The Effective Potential at Finite Temperature

The properites of a QFT at finite temperature in thermodynamic equilibrium can be described by standard statistical mechanics methods. Thermodynamic expectation values are obtained from the partition function, defined in the usual way by [12]

$$\mathcal{Z} = tr(\hat{\rho}) \tag{12}$$

where the trace means to sum over a set of basis states of the Hilbert space and the density operator $\hat{\rho}$ is

$$\hat{\rho} = e^{-\beta(H - \mu_A Q_A)} \ , \tag{13}$$

where $\beta = 1/T$, $H = \int d^3x \, \mathcal{H}$ is the Hamiltonian, and $Q_A = \int d^3x \, j_A^0$ are the conserved charges of the theory.

For a QFT system, the partition function can be expressed in terms of a path integral in nearly the same way as the path integral for standard (zero temperature) QFTs is constructed.[2] Ignoring chemical potentials for now, the result for scalar fields is [12, 14]

$$\mathcal{Z} = \int [\mathscr{D}\phi] \, \exp\left(- \int_0^\beta d\tau \int d^3x \, S_E[\phi] \right) \ , \tag{14}$$

[2]Recall the key formula $\langle \phi_f(t_f) | \phi_i(t_i) \rangle = \langle \phi_f(0) | e^{-iH(t_f - t_i)} | \phi_i(0) \rangle = \int [\mathscr{D}\phi]_{\phi_i}^{\phi_f} \exp(iS[\phi])$.

where $S_E[\phi]$ is the Euclidean action and the sum on configurations runs over classical fields that are periodic in $\tau = it$ with period β: $\phi(\beta, \vec{x}) = \phi(0, \vec{x})$. This periodicity is needed to ensure a trace over bosonic configurations. An analagous result apply to fermions, but now the trace requirement implies that the path integral runs over antiperiodic configurations: $\psi(\beta, \vec{x}) = -\psi(0, \vec{x})$ [12, 14].

With the partition function in hand, thermodynamic expectation values can be calculated in the usual way by inserting the corresponding operator into the integrand of the path integral of Eq. (14). The calculation works just like in standard QFT formulated in terms of path integrals, with the main exception being the requirement of periodicity (or anti-periodicity) in Euclidean time direction. For bosons, this means the mode expansion is [12]

$$\phi(\tau, \vec{x}) = \sqrt{\beta} \sum_{n=\infty}^{\infty} \int \frac{d^3p}{(2\pi)^3} \phi_n(\vec{k})\, e^{i(\omega_n \tau + i\vec{k}\cdot\vec{x})} \ , \tag{15}$$

where the $\omega_n = 2\pi\, n\, T$ are called *Matsubara frequencies*. A similar mode expansion applies to fermions, but now with odd Matsubara frequencies only, $\omega_n = (2n+1)\,\pi\, T$. With these expansions, Feynman diagrams can be calculated with propagators and vertices corresponding to the expansions.

Applying this formalism to a general theory, the one-loop result in Landau gauge is [9]

$$V_{eff}(\phi, T) = V_0(\phi) + V_1(\phi) + \Delta V_1(\phi, T) \ , \tag{16}$$

where V_0 and V_1 are the same as before, and ΔV_1 is the leading thermal correction,

$$\Delta V_1(\phi, T) \ = \ \sum_{i=boson} g_i \frac{T^4}{2\pi^2} J_b(m_i^2/T^2) \ - \sum_{j=fermion} g_i \frac{T^4}{2\pi^2} J_f(m_j^2/T^2) \ , \tag{17}$$

with the boson and fermion thermal functions J_b and J_f given by

$$J_{b/f}(x^2) = \int dt\, t^2 \ln\left(1 \mp e^{-\sqrt{t^2+x^2}}\right) \ . \tag{18}$$

For $x \ll 1$, these functions have the asymptotic forms [16]

$$J_b(x^2) = -\frac{\pi^4}{45} + \frac{\pi^2}{12}x^2 - \frac{\pi}{6}x^3 - \frac{1}{32}x^4 \ln(x^2/a_b) + \mathcal{O}(x^3) \ , \tag{19}$$

$$J_f(x^2) = -\frac{7\pi^4}{360} - \frac{\pi^2}{24}x^2 - \frac{1}{32}x^4 \ln(x^2/a_b) + \mathcal{O}(x^3) \ , \tag{20}$$

with $\ln(a_b) \simeq 5.4076$ and $\ln(a_f) \simeq 2.6351$. For $x \gg 1$, both functions reduce to

$$J_b(x^2) = J_f(x^2) = \left(\frac{x}{2\pi}\right)^{3/2} e^{-x} \left(1 + \frac{15}{8x} + \mathcal{O}(1/x^2)\right) \ . \tag{21}$$

Note the exponential supprression for particles with $m_i \gg T$. Numerically, the asymptotic forms above (expanded to the order shown) work quite well for $x_i \lesssim 2$ and $x_i \gtrsim 2$ respectively.

The physical interpretation of the finite-temperature effective potential is very similar to the zero-temperature version. For a given value of ϕ, it gives the lowest energy configuration for the system among states forced to have $\langle\phi(x)\rangle = \phi$. At the (global) minimum it coincides with the vacuum state of the thermal system, corresponding to the lowest value of the (Helmholtz) *free energy density*,

$$f = \rho - T\,s \ , \tag{22}$$

where ρ is the regular energy density and s is the entropy density. Replacing the regular energy density with the free energy density takes into account the effects of thermal corrections on the equilibrium state of the system. In some cases, the change in the equilibrium state compared to $T = 0$ can be drastic.

1.3 Symmetry Restoration in the SM

Electroweak symmetry breaking in the SM provides an important example of the power of thermal effects. The thermal effective potential (in Landau gauge with $\overline{MS}$ renormalization) is given by the expressions of Eqs. (16,17) with the same contributions as those listed in Eq. (11). At low temperatures, $T \ll v$, we have $x \gg 1$ in the most important thermal functions of Eq. (18) and the effective potential simply reduces to the $T = 0$ version. In contrast, at temperatures much higher than the masses of all the SM particles at a given value of ϕ, we can use the small $x = m_i(\phi)/T$ expansions of the thermal loop functions. Keeping only the leading quadratic corrections, the thermal effective potential becomes

$$V_{eff}(\phi, T) \ \simeq \ -(\mu^2 - D\,T^2)\phi^2 + \frac{\lambda}{2}\phi^4 \tag{23}$$

where

$$D \ \simeq \ \frac{1}{8}\left(2y_t^2 + 3g^2 + g'^2\right) \ . \tag{24}$$

From this, we see that the net coefficient of the quadratic term in V_{eff} becomes positive at large temperatures. When it does, the minimum of the potential shifts to $\phi = 0$ corresponding to no electroweak symmetry breaking at very high T! This is called the *electroweak phase transition*.

2 EWBG: First-Order Electroweak Phase Transtion

We have just seen that the full electroweak gauge invariance becomes manifest at sufficiently high temperatures. Electroweak baryogenesis operates near the phase transition from the unbroken phase to the broken. For the mechanism to work, the phase transition must be *first-order*. When it is, the transition proceeds through the nucleation of bubbles or broken phase within the surrounding plasma of symmetric phase. In this section we study the dynamics of a first-order electroweak phase transition, we discuss what is needed beyond the SM for it to occur, and we describe experimental searches for the corresponding new physics.

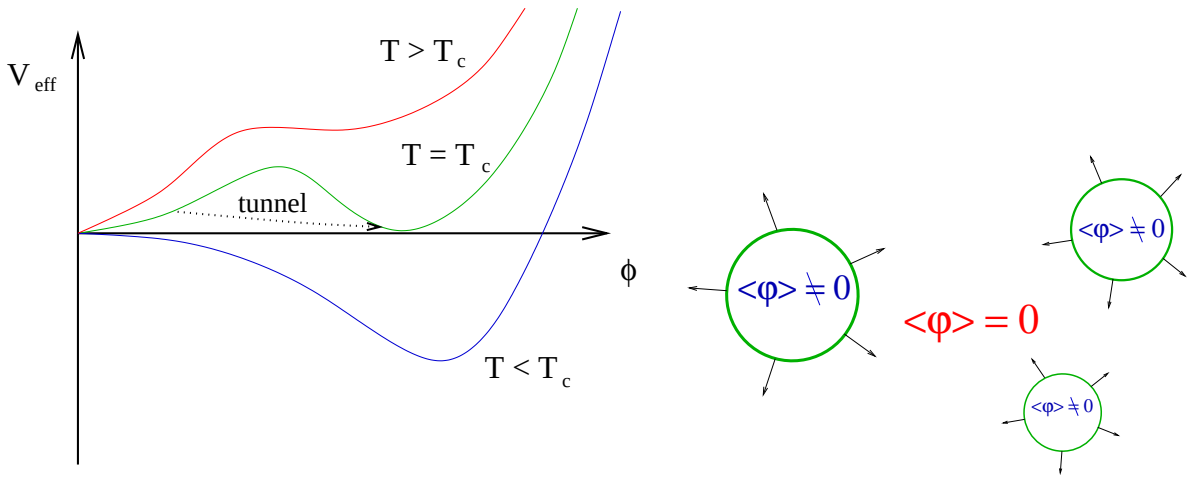

Figure 2: **Left:** Illustration of the form of the temperature evolution of the effective potential needed for a first order phase transition. As T falls below T_c, thermal or quantum transitions to the deeper global minimum can occur. **Right:** Bubbles of broken phase expanding with the plasma of symmetric phase resulting from these transitions.

2.1 Transition Estimates

The structure of the thermal effective potential for a first-order phase transition is shown in the left panel of Fig. 2. At very high temperatures, the global minimum of the thermal potential lies at the origin, $\phi = 0$. As the temperature falls, a second symmetry breaking local minimum forms away from the origin, and becomes degenerate with the origin at the *critical temperature* T_c. Cooling further, $T < T_c$, the second symmetry breaking minimum grows deeper than origin and becomes to the equilibrium configuration of the system. However, the system is trapped at the origin at this time by the barrier separating them. Transitions to the symmetry breaking minimum at $T < T_c$ occur through quantum tunnelling or thermal fluctuations, whichever is faster. In either case, the transition proceeds through the nucleation of a finite-sized bubble of broken phase within the surrounding symmetric phase. If the bubble is large enough, it expands and grows until it coalesces with other bubbles of broken phase. This is illustrated in the right panel of Fig. 2.

Most of the properties of the electroweak phase transition (EWPT) relevant to EWBG can be computed (or estimated) from the thermal effective potential. The full thermal effective potential is complicated and usually calculated numerically in realistic studies. Even so, a useful approximate analytic understanding can be obtained by studying the leading terms that contribute to it. Expanding the thermal corrections to quartic order in $x_i = m_i/T$, and keeping only the contributions from particles with $m_i/T \lesssim 2$ that avoid strong exponential suppression, the potential in the SM and many other theories can be written in the form [9, 16]

$$V_{eff}(\phi, T) \simeq D(T^2 - T_0^2)\phi^2 - ET\phi^3 + \frac{\overline{\lambda}}{2}\phi^4 \,, \tag{25}$$

where the parameters D, T_0, E, and $\overline{\lambda}$ are positive and vary slowly with temperature T. Note that relative to Eq. (23), we have expanded to higher order in $x_i = m_i/T$. In the SM at high temperature, they are given by

$$\begin{aligned} DT_0^2 &= \mu^2 + \dots , & \overline{\lambda} &= \lambda + \dots \\ D &= \frac{1}{8}\left(2y_t^2 + 3g^2 + g'^2\right) + \dots , & E &= \frac{1}{2\sqrt{2}\pi}\left[2g^3 + (g^2+g'^2)^{3/2}\right] + \dots \end{aligned} \tag{26}$$

The extrema of the simplified thermal potential are

$$\phi = 0 , \quad \frac{1}{2\overline{\lambda}}\left[3ET \pm \sqrt{9E^2T^2 - 16\overline{\lambda}D(T^2 - T_0^2)}\right] . \tag{27}$$

Note that only real and non-negative solutions correspond to physically relevant extrema, based on how we defined the classical field ϕ. For $E \to 0$, the $\phi = 0$ extremum is either the global minimum or a local maximum, and therefore a first-order phase transition is only possible with non-zero E. When a first-order transition does occur, it is standard practice to characterize the *strength* of the transition by the ratio of the field value at the non-zero minimum to the temperature at the critical temperature, when $V(0, T_c) = V(\phi_c, T_c)$ Using approximate form of Eq. (25), the result is

$$\frac{\phi_c}{T_c} = \frac{E}{\overline{\lambda}} . \tag{28}$$

We will see below that successful EWBG requires $\phi_c/T_c \gtrsim 1$. Since $\overline{\lambda} \simeq \lambda$ is mostly fixed by the observed Higgs mass, this condition on the phase transition implies a particle physics requirement for the E coefficient.[3]

2.2 New Physics for a Strong Transition

Detailed studies of the electroweak phase transition in the SM find that it is a smooth crossover for $m_h = 125$ GeV [5]. Therefore EWBG does not operate in the minimal SM. However, if the SM is extended with new fields that couple significantly to the Higgs, a strong first order phase transition is possible. There are two main approaches to this. The first is couple new bosonic fields to the Higgs to modify the thermal effective potential through loop effects. In the second, new physics connected to the SM Higgs field modifies the effective potential at tree-level. We give examples of both approaches here [11].

In the loop approach to generating a strongly first order electroweak phase transition, them primary effect comes from loops of new bosons coupled to the Higgs. This can be understood from the way the thermal functions of Eqs. (19) contributes to the cubic E

[3] The condition $\phi_c/T_c \gtrsim 1$ should be used with some caution since this quantity is formally gauge dependent [17, 18].

coefficient in the simplified form of Eq. (25). A simple explicit example is given by a new scalar X with g_X internal degrees of freedom and interactions [19]

$$-\mathscr{L} \supset M_X^2|X|^2 + \frac{K}{6}|X|^4 + Q\,|X|^2|H|^2 \ . \tag{29}$$

The third term above is called the *Higgs portal* operator and is allowed no matter what gauge charges X might have. As long as X does not develop a VEV, its physical mass as a function of the Higgs background value is

$$m_X^2 = M_X^2 + Q\phi^2 \ . \tag{30}$$

For $T \gg m_X$, the x^3 term in Eq. (19) leads to the contribution

$$\Delta V_{eff} = -\frac{g_X}{12\pi}T(M_X^2 + Q\phi^2)^{3/2} \ . \tag{31}$$

For $M_X^2 \to 0$, this contributes to the cubic term with coefficient $\Delta E = g_X Q^{3/2}/12\pi$, potentially driving a strongly first order electroweak phase transition for large g_X or Q. Note as well that this approach only works with bosons, since there is no corresponding x^3 term in Eq. (20).

This approach to the EWPT faces a significant challenge. The cubic term arises specifically in the limit of small M_X^2. When this mass parameter is large, the expression of Eq. (31) can be expanded reliably in powers of $(Q\phi^2/M_X^2)$ and no effective cubic term is generated. In fact, this challenge is made even worse when higher-order thermal corrections are included. In the same way that thermal effects alter the effective potential, they also modify the effective masses of particles in the plasma.[4] Resumming these so-called *daisy corrections* to leading order, they add a new term to the effective potential [9, 20]:

$$\Delta V_1^{daisy} = -\frac{T}{12}\sum_{i=boson'} g_i \left[\overline{m}_i^3(\phi,T) - m_i^3(\phi)\right] \ , \tag{32}$$

where the sum runs over scalars and longitudinal vectors, and $\overline{m}_i^2(\phi,T)$ is the thermally corrected mass,

$$\overline{m}_i^2(\phi,T) = m_i^2(\phi) + \Pi(T) \ , \tag{33}$$

and $\Pi(T) \sim (T^2 + \ldots) \geq 0$ is the thermal self-energy correction. Going back to our scalar example, this correction changes the potentially cubic term to

$$\Delta V_{eff} = -\frac{g_X}{12\pi}T\left(M_X^2 + \Pi_X(T) + Q^2\phi^2\right)^{3/2} \tag{34}$$

To obtain a sufficiently strongly first order phase transition, the mass parameter M_X^2 must often be negative to cancel the positive thermal mass correction to yield an effective cubic term, and this tends to drive the physical mass of the new scalar to small values.

[4]Thermal effects at high T lead to the breakdown of perturbation theory [9]. Daisy resummation postpones this a little.

To illustrate the tree-level approach, consider a new gauge singlet scalar field N with couplings [21]

$$-\mathscr{L} \supset m_N^2 N^2 + A_N N^3 + \lambda_N N^4 + (A_H N + \kappa_H N^2)|H|^2 + \dots \tag{35}$$

If both scalar fields develop VEVs they will mix with each other through the A_H and κ terms. When they do, it is often convenient to parametrize the field values using polar coordinates

$$\langle H^0 \rangle = \varphi \cos\alpha \ , \qquad \langle N \rangle = \varphi \sin\alpha \ , \tag{36}$$

for some mixing angle α and field parameter φ. Expanding the potential in these parameters leads to a tree-level potential with cubic terms. The new scalar can also contribute to loop-level cubic terms as above. A diverse range of phase transition dynamics can occur in this simple model, including a strongly first order electroweak transition.

2.3 Bubble Dynamics

As the universe cools below the critical temperature, it remains stuck initially at the electroweak origin. The electroweak phase transition only occurs some time later when bubbles of broken phase are nucleated by thermal or quantum tunnelling, and specifically when the transition rate grows larger than the Hubble rate. It is conventional to define the *nucleation temperature* T_n and field minimum ϕ_n as the values when this occurs. The ratio ϕ_n/T_n gives a better characterization of the strength of the phase transition than ϕ_c/T_c we used earlier. However, ϕ_c/T_c is much easier to compute and tends to be similar or smaller than ϕ_n/T_n.

The thermal and quantum nucleation rates can be estimated from thermal effective potential. Thermal transitions correspond to thermal fluctuations over the potential barrier. Their rate per unit volume has the form [22]

$$\Gamma_3 \simeq T^4 e^{-S_3[\varphi_3]/T} \ , \tag{37}$$

where S_3 is the 3-dimensional Euclidean action

$$S_3[\varphi_3] = \int d^3x \left[\frac{1}{2}(\vec{\nabla}\varphi_3)^2 + V_{eff}(\varphi_3/\sqrt{2}, T) \right] \ . \tag{38}$$

It is to be computed specifically for the time independent *thermal bounce solution* φ_3 connecting the $\phi = 0$ and $\phi \neq 0$ phases. For the spherically symmetric bounce, which usually dominates the rate, φ_3 is the solution of

$$\partial_r^2 \varphi_3 + \frac{2}{r}\partial_r \varphi_3 = +\frac{\partial V_{eff}}{\partial \varphi_3} \ , \tag{39}$$

with boundary conditions

$$\varphi_b(r \to \infty) \to 0 \ , \qquad \partial_r \varphi_b(r = 0) = 0 \ . \tag{40}$$

Similarly, the quantum tunnelling rate per volume is obtained from [23, 24]

$$\Gamma_4 \simeq m_W^4 e^{-S_4[\varphi_4]} , \tag{41}$$

with S_4 now the 4-dimensional Euclidean action

$$S_4[\varphi_4] = \int d^4x_E \left[\frac{1}{2}\left(\frac{d\varphi_4}{dt}\right)^2 + \frac{1}{2}(\vec{\nabla}\varphi_4)^2 + V_{eff}(\varphi_4/\sqrt{2}, T) \right] , \tag{42}$$

where now φ_4 is the 4-dimensional Euclidean bounce solution connecting the phases. Note the bounce for both mechanisms is computed using the effective potential. A very nice tool for doing this numerically is CosmoTransitions [25].[5] In addition to controlling the nucleation rate, the bounce solution also gives the field profile of the bubble wall as it transitions from $\phi \neq 0$ inside to $\phi = 0$ outside.

2.4 Experimental Tests

Higgs tests, direct searches, gravitational waves...

3 EWBG: Baryon Creation near Bubbles

Electroweak bubbles are a necessary ingredient for EWBG, but they are only the stage upon which the intricate drama of baryon creation takes place. A schematic overview of the process is shown in Fig. 1. Interactions in the vicinity of the advancing bubble wall generate temporary charge asymmetries outside the bubble that bias the sphalerons to create more baryons than antibaryons. The baryons made this way are then swept up into the interior where they are (nearly) stable. Computing the baryon asymmetry from EWBG is very challenging and still very much a work in progress. We only give a broad overview here.

The guiding relation for the calculation of the EWBG baryon asymmetry is the evolution equation for B due to sphalerons, whose rates are modified very slightly in the presence of fermion densities. The leading effect can be derived from the property that in (or close to) thermodynamic equilibrium, the ratio of transition rates between states with free energies F_+ and F_- is

$$\frac{\Gamma_+}{\Gamma_-} = e^{-\Delta F/T} , \tag{43}$$

where $\Delta F = F_+ - F_-$. This relation is needed to ensure that the net transition rates balance out to zero in equilibrium. Applying this very general relation to the weak sphalerons, we

[5] See also Ref. [26] for a related tool.

have [8, 27]

$$\begin{aligned}\frac{dn_B}{dt} &= -n_g(\Gamma_- - \Gamma_+) \\ &= -n_g\Gamma_{sp}(1 - e^{-\Delta F/T}) \\ &= -n_g\Gamma_{sp}\sum_i (3\mu_{Q_i} + \mu_{\ell_i})/T\end{aligned} \tag{44}$$

where we have used $\Delta B = n_g$ in each sphaleron transition, $\Gamma_- \simeq \Gamma_{sp}$ (*i.e.* the sphaleron rate neglecting fermions), and $\Delta F = \sum_i (3\mu_{Q_i} + \mu_{\ell_i})$ as the small change in free energy from the sphaleron transition. Rearranging this expression, it becomes

$$\frac{dn_B}{dt} = \Gamma_{sp}\sum_a A_a \left(\frac{\mu_a}{T}\right) - n_g\, C\, \frac{\Gamma_{sp}}{T^3}\, n_B \ , \tag{45}$$

where A_a and C are dimensionless, and $n_B \simeq \sum_i (2\mu_{Q_i} + \mu_{u_i} + \mu_{d_i})T^3/6$. The first term above is a linear combination of chemical potentials independent from μ_B, and it acts as a source for B creation by sphalerons when it is non-zero. The second term presents a challenge, since it tends to wash out any B charge that has been created.

There are three steps in computing the EWBG baryon density with Eq. (45):

1. Derive sources terms for μ_a from CP violation in the bubble walls.
2. Incorporate these in diffusion and transfer equations to find the creation, evolution, and transport of the charges corresponding to the μ_a.
3. Apply Eq. (45) to find the baryon density created by the source term from the μ_a, and check that it is not washed out.

All three steps present theoretical challenges.

3.1 Bubbles and Charges

Bubble wall profile, Fig. 3. Define wall-frame coordinate $z = x - v_w t$.

$$\phi(z) = \frac{\phi_n}{2}\left[1 - \tanh\left(\frac{z}{L_w}\right)\right] \tag{46}$$

3.2 CPV Sources

3.3 Experimental Tests

EDM searches, direct searches, precision Higgs...

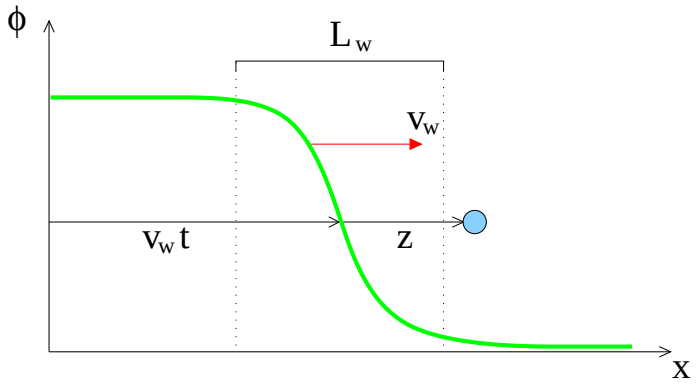

Figure 3: Bubble wall profile of width L_w moving right at speed v_w. The blue dot represents a random spot in front of the wall, and illustrates our coordinate system.

References

[1] V. A. Kuzmin, V. A. Rubakov and M. E. Shaposhnikov, "On the Anomalous Electroweak Baryon Number Nonconservation in the Early Universe," Phys. Lett. **155B**, 36 (1985). doi:10.1016/0370-2693(85)91028-7

[2] M. E. Shaposhnikov, "Possible Appearance of the Baryon Asymmetry of the Universe in an Electroweak Theory," JETP Lett. **44**, 465 (1986) [Pisma Zh. Eksp. Teor. Fiz. **44**, 364 (1986)].

[3] M. E. Shaposhnikov, "Baryon Asymmetry of the Universe in Standard Electroweak Theory," Nucl. Phys. B **287**, 757 (1987). doi:10.1016/0550-3213(87)90127-1

[4] A. G. Cohen, D. B. Kaplan and A. E. Nelson, Ann. Rev. Nucl. Part. Sci. **43**, 27 (1993) doi:10.1146/annurev.ns.43.120193.000331 [hep-ph/9302210].

[5] M. D'Onofrio and K. Rummukainen, Phys. Rev. D **93**, no. 2, 025003 (2016) doi:10.1103/PhysRevD.93.025003 [arXiv:1508.07161 [hep-ph]].

[6] M. B. Gavela, P. Hernandez, J. Orloff and O. Pene, "Standard model CP violation and baryon asymmetry," Mod. Phys. Lett. A **9**, 795 (1994) doi:10.1142/S0217732394000629 [hep-ph/9312215].

[7] M. B. Gavela, P. Hernandez, J. Orloff, O. Pene and C. Quimbay, Nucl. Phys. B **430**, 382 (1994) doi:10.1016/0550-3213(94)00410-2 [hep-ph/9406289].

[8] A. Riotto, "Theories of baryogenesis," hep-ph/9807454.

[9] M. Quiros, "Finite temperature field theory and phase transitions," hep-ph/9901312.

[10] J. M. Cline, "Baryogenesis," hep-ph/0609145.

[11] D. E. Morrissey and M. J. Ramsey-Musolf, "Electroweak baryogenesis," New J. Phys. **14**, 125003 (2012) doi:10.1088/1367-2630/14/12/125003 [arXiv:1206.2942 [hep-ph]].

[12] J. I. Kapusta and C. Gale, "Finite-temperature field theory: Principles and applications," *Cabridge, UK: Cambridge University Press, 2006 442p.*

[13] R. H. Brandenberger, Rev. Mod. Phys. **57**, 1 (1985). doi:10.1103/RevModPhys.57.1

[14] J. Polchinski, "String theory. Vol. 1: An introduction to the bosonic string," *Cambridge, UK: Cambridge University Press (1998) 424 p.*

[15] E. J. Weinberg and A. q. Wu, "Understanding Complex Perturbative Effective Potentials," Phys. Rev. D **36**, 2474 (1987). doi:10.1103/PhysRevD.36.2474

[16] G. W. Anderson and L. J. Hall, "The Electroweak phase transition and baryogenesis," Phys. Rev. D **45**, 2685 (1992). doi:10.1103/PhysRevD.45.2685

[17] H. H. Patel and M. J. Ramsey-Musolf, "Baryon Washout, Electroweak Phase Transition, and Perturbation Theory," JHEP **1107**, 029 (2011) doi:10.1007/JHEP07(2011)029 [arXiv:1101.4665 [hep-ph]].

[18] M. Garny and T. Konstandin, "On the gauge dependence of vacuum transitions at finite temperature," JHEP **1207**, 189 (2012) doi:10.1007/JHEP07(2012)189 [arXiv:1205.3392 [hep-ph]].

[19] T. Cohen, D. E. Morrissey and A. Pierce, "Electroweak Baryogenesis and Higgs Signatures," Phys. Rev. D **86**, 013009 (2012) doi:10.1103/PhysRevD.86.013009 [arXiv:1203.2924 [hep-ph]].

[20] D. Curtin, P. Meade and H. Ramani, "Thermal Resummation and Phase Transitions," arXiv:1612.00466 [hep-ph].

[21] S. Profumo, M. J. Ramsey-Musolf and G. Shaughnessy, "Singlet Higgs phenomenology and the electroweak phase transition," JHEP **0708**, 010 (2007) doi:10.1088/1126-6708/2007/08/010 [arXiv:0705.2425 [hep-ph]].

[22] A. D. Linde, "Decay of the False Vacuum at Finite Temperature," Nucl. Phys. B **216**, 421 (1983) Erratum: [Nucl. Phys. B **223**, 544 (1983)]. doi:10.1016/0550-3213(83)90293-6, 10.1016/0550-3213(83)90072-X

[23] S. R. Coleman, "The Fate of the False Vacuum. 1. Semiclassical Theory," Phys. Rev. D **15**, 2929 (1977) Erratum: [Phys. Rev. D **16**, 1248 (1977)]. doi:10.1103/PhysRevD.15.2929, 10.1103/PhysRevD.16.1248

[24] C. G. Callan, Jr. and S. R. Coleman, "The Fate of the False Vacuum. 2. First Quantum Corrections," Phys. Rev. D **16**, 1762 (1977). doi:10.1103/PhysRevD.16.1762

[25] C. L. Wainwright, "CosmoTransitions: Computing Cosmological Phase Transition Temperatures and Bubble Profiles with Multiple Fields," Comput. Phys. Commun. **183**, 2006 (2012) doi:10.1016/j.cpc.2012.04.004 [arXiv:1109.4189 [hep-ph]], https://pypi.python.org/pypi/cosmoTransitions.

[26] J. E. Camargo-Molina, B. O'Leary, W. Porod and F. Staub, "**Vevacious**: A Tool For Finding The Global Minima Of One-Loop Effective Potentials With Many Scalars," Eur. Phys. J. C **73**, no. 10, 2588 (2013) doi:10.1140/epjc/s10052-013-2588-2 [arXiv:1307.1477 [hep-ph]].

[27] L. P. Csernai and J. I. Kapusta, "Nucleation of relativistic first order phase transitions," Phys. Rev. D **46**, 1379 (1992). doi:10.1103/PhysRevD.46.1379

[28] M. E. Peskin and D. V. Schroeder, "An Introduction To Quantum Field Theory," *Reading, USA: Addison-Wesley (1995) 842 p*

[29] C. P. Burgess and G. D. Moore, "The standard model: A primer," *Cambridge, UK: Cambridge Univ. Pr. (2007) 542 p*

[30] C. Patrignani *et al.* [Particle Data Group], "Review of Particle Physics," Chin. Phys. C **40**, no. 10, 100001 (2016);
http://pdg.lbl.gov/

[31] E. Eichten, K. Gottfried, T. Kinoshita, K. D. Lane and T. M. Yan, "Charmonium: Comparison with Experiment," Phys. Rev. D **21**, 203 (1980). doi:10.1103/PhysRevD.21.203

[32] R. Gupta, "Introduction to lattice QCD: Course," hep-lat/9807028.

[33] U. Wiese, "An Introduction to Lattice Field Theory," www.itp.uni-hannover.de/saalburg/Lectures/wiese.pdf.

[34] H. Georgi, "Weak Interactions,"
http://www.people.fas.harvard.edu/ hgeorgi/weak.pdf

[35] D. B. Kaplan, "Five lectures on effective field theory," [nucl-th/0510023].

[36] A. Pich, "Effective field theory: Course," [hep-ph/9806303].

[37] D. E. Morrissey, "PHYS 528 Notes #4,"
http://trshare.triumf.ca/ dmorri/Teaching/PHYS528-2014/notes-04.pdf

[38] J. F. Donoghue, E. Golowich and B. R. Holstein, "Dynamics of the standard model," Camb. Monogr. Part. Phys. Nucl. Phys. Cosmol. **2**, 1 (1992) [Camb. Monogr. Part. Phys. Nucl. Phys. Cosmol. **35** (2014)].

[39] C. Csáki and P. Tanedo, 2013 European School of High-Energy Physics, Paradfurdo, Hungary, 5 - 18 Jun 2013, pp.169-268 (CERN-2015-004) doi:10.5170/CERN-2015-004.169 [arXiv:1602.04228 [hep-ph]].